Research Article

Characterization of *OAZ1* and its potential functions in goose follicular development

CrossMark

Bo Kang [a,b,*,1], Dongmei Jiang [a,b,*,1], Hui He [a], Rong Ma [a], Zhixin Yi [a], Ziyu Chen [a]

[a] *College of Animal Science and Technology, Sichuan Agricultural University, Chengdu, Sichuan 611130, People's Republic of China*
[b] *Farm Animal Genetic Resources Exploration and Innovation Key Laboratory of Sichuan Province, Sichuan Agricultural University, Chengdu, Sichuan 611130, People's Republic of China*

ARTICLE INFO

ABSTRACT

Background: Ornithine decarboxylase antizyme 1 (OAZ1) is an important regulator of polyamine synthesis and uptake. Our previous studies indicated that high *OAZ1* expression in the ovaries of laying geese is responsible for poor egg production. In the present study, the molecular characterization of goose *OAZ1* gene was analyzed, as well as the expression profile in various follicular tissues.
Results: An 873-bp cDNA sequence of the *OAZ1* gene (Accession No. KC845302) with a +1 frameshift site (+175T) was obtained. The sequence consisted of a 652-bp two overlapping open reading frames (a putative protein with 216 amino acids). The OAZ domain, OAZ signature and OAZ super family domain were prominent conserved regions among species. As the follicle size increased, *OAZ1* abundance showed an increasing trend during follicular development, while it decreased during follicular regression. The level of *OAZ1* mRNA expression was the lowest in the fifth largest preovulatory follicle, and was 0.65-fold compared to the small white follicle ($P < 0.05$). *OAZ1* mRNA expression in the largest preovulatory and postovulatory follicle was 2.11- and 2.49-fold compared to the small white follicle, respectively ($P < 0.05$).
Conclusions: The goose *OAZ1* structure confirms that OAZ1 plays an important role in ornithine decarboxylase-mediated regulation of polyamine homeostasis. Our findings provide an evidence for a potential function of OAZ1 in follicular development, ovulation and regression.

1. Introduction

Polyamines (*i.e.,* putrescine, spermidine and spermine) play important roles in many biological processes, including cell growth, differentiation and apoptosis [1,2]. Polyamines have recently been shown to be essential for successful reproduction functions in animals, including the regulation of spermatogenesis and oogenesis, embryogenesis, implantation, embryonic and gonadal development [3,4,5,6]. Intracellular polyamine content is regulated tightly by concerted biosynthesis and uptake mechanisms, as well as by degradation and efflux processes [7]. Ornithine decarboxylase (ODC), which catalyzes decarboxylation of L-ornithine to form putrescine, is the first rate-limiting enzyme in the polyamine biosynthesis pathway. ODC expression is regulated strictly at multiple levels including transcription, post-transcriptional processing, change in translational efficiency, and altered stability of the protein [8,9].

Ornithine decarboxylase antizyme 1 (OAZ1), which targets ODC for ubiquitin-independent proteasome degradation and inhibits polyamine influx process, is considered as a negative regulator of intracellular polyamines [10,11]. *OAZ1* expression is also regulated at the translational level by polyamines [12]. *OAZ1* transcript exists with two overlapping open reading frames (ORFs) [13]. A unique +1 ribosomal frameshift mechanism is needed for translation of a fully functional OAZ1 protein [14,15]. Increased polyamine levels induce translation of the full-length functional *OAZ1* by bypassing an in-frame stop codon on *OAZ1* mRNA and by relieving the translational repression effect mediated through the N-terminal fragment of *OAZ1* [16,17].

Our previous study reported that the level of *OAZ1* mRNA expression was significantly higher in the ovaries of laying than pre-laying geese [18]. It suggested that higher expression of *OAZ1* disrupted polyamine homeostasis by inhibiting ODC activity, suppressed follicular development, and decreased egg production. An et al. [19] reported a higher level of *OAZ1* gene expression in ovarian tissues of polytocous compared to monotocous goats [19]. Li et al. [4] suggested that OAZ was involved in the gonadal development of small abalone. These results indicate that OAZ1 plays an important role in regulating

* Corresponding authors.
E-mail addresses: bokang@sicau.edu.cn (B. Kang), jiangdm@sicau.edu.cn (D. Jiang).
1 Bo Kang and Dongmei Jiang contributed equally to this work.
Peer review under responsibility of Pontificia Universidad Católica de Valparaíso.

reproductive function, follicular development and ovulation. To gain more insight into the function of OAZ1 in follicular development, we cloned *OAZ1* coding sequence of the Sichuan white goose (*Anser cygnoides*), and examined *OAZ1* expression profiles in various follicles and ovarian stroma.

2. Materials and methods

2.1. Animals and sample collection

All procedures in this study involving animals were in accordance with ethical standards of the Animal Ethics Committee of the College of Animal Science and Technology, Sichuan Agricultural University. Adult Sichuan white geese (*A. cygnoides*), which reach sexual maturation at approximately 6 months, were obtained from the Experimental Farm of Waterfowl Breeding in Sichuan Agricultural University (Ya'an, China). All of experimental geese hatched on the same day were kept under conditions of natural light and temperature. Geese were fed standard chow and water *ad libitum*. Laying geese (n = 5) were euthanized by cervical dislocation about 8 h after the first or second oviposition in an egg sequence. Ovaries along with the ovarian follicles were quickly removed and processed. Ovarian stroma and follicles at different stages of development including the small white follicle (SWF), small yellow follicle (SYF), preovulatory hierarchal follicle (F5, F4, F3, F2, and F1) and postovulatory follicle (POF1, POF2, POF3 and POF4) according to their color and stages of differentiation were collected for RNA isolation as previously described [20]. All of follicles were operated on transversely along the stigma to completely eliminate the yolk material, and washed using the ice-cold sterile saline. Walls of ovarian follicles (including the theca and granulosa layer) were isolated for RNA extraction.

2.2. Cloning of goose OAZ1 gene

Total RNA was isolated from ovary tissues using RNAiso Plus and cDNAs were synthesized using PrimeScript® RT reagent Kit from Takara (China) according to the manufacturer's protocol. The cDNA newly synthesized was stored at -20°C until further analysis. Based on the *OAZ1* cDNA sequence of *Anas platyrhynchos* (GenBank accession no. NM_001289841) and *Gallus gallus* (NM_204916), the gene-specific primer named *OAZ1*-L was designed to amplify the full coding region of *OAZ1* using the Oligo 7.0 (forward: 5′-AGGGTTTCGGGGTTCGGACCA-3′, reverse: 5′-TTGCACAACCACAACATGCGCAC-3′). The PCR amplification reaction was performed with the following protocol using a Bio-Rad thermal cycler (Bio-Rad, USA): 95°C pre-denature for 5 min, followed by 35 cycles of 30 s at 95°C, annealing for 30 s at 63°C, extension at 72°C for 60 s; final extension for 10 min at 72°C. PCR products were gel-purified and ligated into the pGEM-T Easy Vector (Promega, USA), which were transformed into *E. coli* DH5α competent cells. Positive clones that contained expected-size inserts were screened by colony PCR and then sequenced by Sangon Biotech (Shanghai, China).

2.3. Bioinformatic analysis of goose OAZ1 gene

The nucleotide sequence of the *OAZ1* gene has been deposited in the NCBI/GenBank Data Libraries under the accession number KC845302. Sequence analyses were performed using NCBI website (http://www.ncbi.nlm.nih.gov). The Protparam (http://web.expasy.org/protparam/) web-based program was employed to predict the physiochemical properties of the OAZ1 protein. The domains of the OAZ1 putative amino acid were predicted using the Phyre2 program (http://www.sbg.bio.ic.ac.uk/phyre2). A phylogenetic tree was constructed using the ClustalX2 and MEGA 5.2 program based on the neighbor-joining method with 1000 bootstrap replicates [21].

2.4. Quantitative real-time PCR

As mentioned above, total RNAs were extracted from ovarian stroma and follicular tissues, and cDNAs were synthesized using a PrimeScript™ RT reagent Kit with a gDNA Eraser (Takara, China). Quantitative real-time PCR (qRT-PCR) employed to measure *OAZ1* mRNA expression profiles in various tissues was performed in a CFX96 (Bio-Rad, USA) using SYBR® Premix Ex Taq™ (Takara, China). The following primers were used: *OAZ1* (forward: 5′-CAGGTGGGCGAGGGAATAGT-3′, reverse: 5′-GCATCTGTAAGCCTTGACTGGAC-3′); glyceraldehyde-3-phosphate dehydrogenase *(GAPDH)* (forward: 5′-GTGGTGCAAGAGGCATTGCTGAC-3′, reverse: 5′-GCTGATGCTCCCATGTTCGTGAT-3′). The amplification was performed in a total volume of 25 μL, containing 0.5 μL of cDNA, 12.5 μL of 2 xSYBR® Premix Ex Taq™ (Takara, China), 0.5 μL of 10 mmol/L of each primer, and 11 μL of nuclease-free water. The qRT-PCR program was 95°C pre-denature for 5 min, followed by 40 cycles of 95°C for 30 s, 65°C for 30 s and 72°C for 30 s, and then a melting curve was performed. Starting temperature was 6°C and increasing by 0.5°C ever 10 s to determine the primers specificity. Threshold and Ct (threshold cycle) values were determined automatically by the CFX Manager™ Software, using default parameters. The comparative cycle threshold ($2^{-\Delta\Delta Ct}$ method) was used to analyze levels of *OAZ1* mRNA expression. Levels of *OAZ1* mRNA expression were normalized against *GAPDH* and expressed as arbitrary units (AU). The relative quantization of mRNA expression was performed in three replicates for each sample.

2.5. Statistical analysis

All the experiments were statistically analyzed by a one-way analysis of variance (ANOVA) using SAS 9.1 statistical software for Windows (SAS Institute Inc., Cary, NC, USA). Statistically significant results by ANOVA were further analyzed by Duncan's multiple range tests. A P value <0.05 was considered statistically significant. Error bars in the graph were generated using mean ± standard error of mean (SEM) values.

3. Results

3.1. Cloning and sequence analysis of goose OAZ1

Based on PCR amplification and sequence analysis, an 873-bp cDNA sequence of the *OAZ1* gene was cloned from the Sichuan white goose. The nucleotide sequence of *OAZ1* was deposited in the GenBank database with accession number of KC845302. The sequence consisted of a 31-bp 5′ untranslated region (UTR), a 190-bp 3′ UTR and a 652-bp two overlapping ORFs. The first short ORF1 with a translational start codon and a stop codon at +175 frameshift site consisted of 177 nucleotides and encoded a putative protein with 58 amino acids. The second short ORF2, which encoded most of the protein but lacked a start codon, consisted of 477 nucleotides and encoded a putative protein with 158 amino acids. A functional, full-length ORF consisted of 652 nucleotides and encoded a putative protein with 216 amino acids (Fig. 1). The homology analyses indicated that the *OAZ1* coding sequence of the goose shared 99, 99, 87 and 80% sequence similarity with the *OAZ1* genes of *A. platyrhynchos* (NM_001289841), *G. gallus* (NM_204916), *Homo sapiens* (NM_004152) and *Mus musculus* (NM_008753), respectively.

3.2. OAZ1 protein structural prediction and phylogenetic analysis

To validate the conserved domain, a multiple-sequence alignment was performed using the ClustalX2 program (Fig. 2). The predicted amino acid sequence of the functional, full-length OAZ1 exhibited 99, 99, 82 and 75% similarity to OAZ1 amino acid sequences from *A. platyrhynchos* (NP_001276770), *G. gallus* (NP_990247), *H. sapiens* (NP_004143) and *M. musculus* (NP_032779), respectively. The analysis
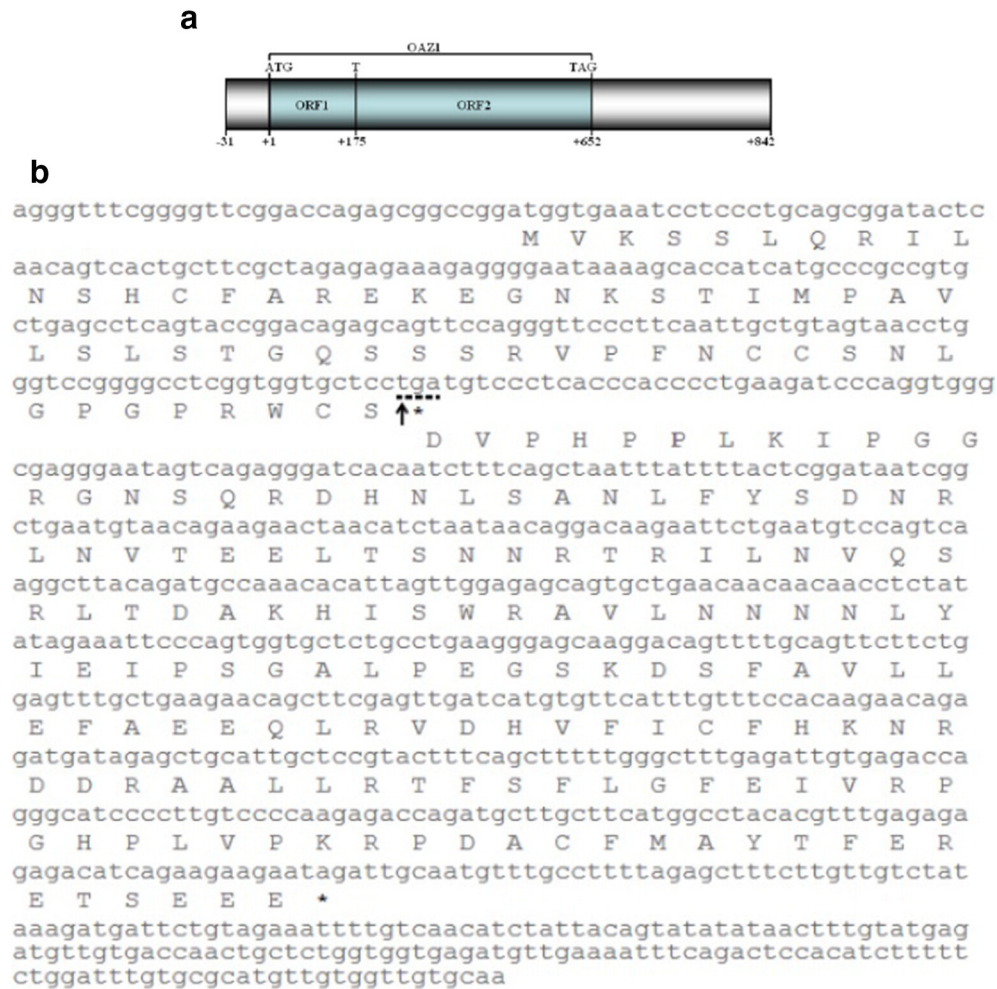
a

b

Fig. 1. Schematic representation of the ORFs of the goose *OAZ1* mRNA. (a) Schematic diagram of the two ORFs. A start codon (ATG), +1 frameshift site (T) and a stop codon (TGA) of the functional full-length *OAZ1* are indicated, as well as ORF1 and ORF2 positions. (b) Deduced amino acid sequence of the *OAZ1* mRNA. (↑) + 1 frameshift site and (*) stop codon.
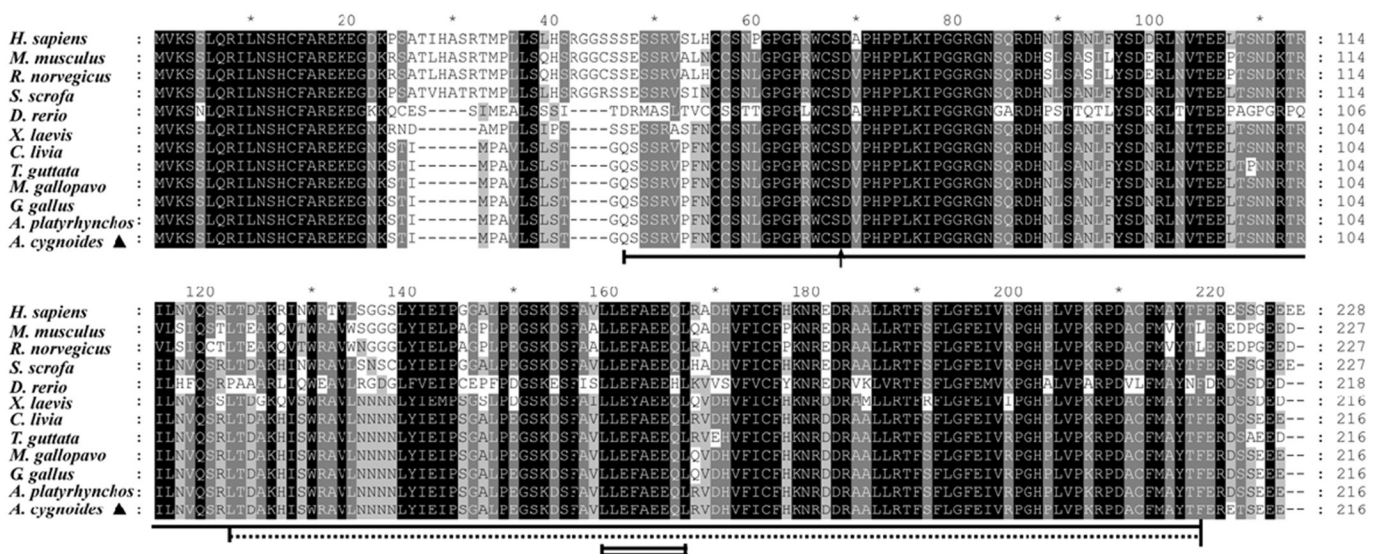

Fig. 2. Comparison between amino acid sequences of OAZ1 from *A. cygnoides* and the other known OAZ1 proteins using the Lasergene MegAlign program. The single line indicates a predicted OAZ domain (position: Q47–F218); the double lines denotes an OAZ signature (position: L159–L167); and the dotted line indicates an OAZ super family domain (position: L122–F218). The position of the +1 frameshift site is marked by an arrow (↑). Accession numbers for sequences used in this alignment: *A. cygnoides* (KC845302), *A. platyrhynchos* (NP_001276770), *Columba livia* (NP_001276803), *G. gallus* (NP_990247), *Taeniopygia guttata* (NP_001166235), *Meleagris gallopavo* (NP_001278810), *H. sapiens* (NP_004143), *Sus scrofa* (NP_001116466), *M. musculus* (NP_032779), *Rattus norvegicus* (NP_620781), *D. rerio* (NP_919413) and *Xenopus laevis* (NP_001080045).

of the physicochemical properties of the OAZ1 protein showed that the molecular formula of OAZ1 was $C_{1068}H_{1680}N_{316}O_{321}S_9$, and that the OAZ1 protein had a molecular mass of 24.37 kDa. The theoretical pI of the OAZ1 protein was 8.25. The instability coefficient of the OAZ1 protein was 58.46, and its average hydrophobicity was -0.47. The subcellular distribution of the OAZ1 protein was predicted to be 39.1% in mitochondria, 26.1% in cell nuclei, 13.0% in cytoplasm, 13.0% extracellular (including cell wall), and 8.7% in the cytoskeleton. The domains analysis predicted the following structural features in the OAZ1 protein: an OAZ domain located from Gln47 to Phe218, the OAZ signature located from Leu159 to Leu167, and OAZ super family domain located from Leu122 to Phe218 (Fig. 2). The protein sequence comparison also showed that two conserved regions are present in OAZ1 sequences of these species. The first 23 amino acids constituted the first conserved region. The second region, which included the OAZ domain, signature and super family domain, was prominent and determined the molecular function of the OAZ. The phylogenetic analysis showed that the goose OAZ1 sequence was most similar to avian species, especially *A. platyrhynchos* (Fig. 3).

3.3. Expression of OAZ1 mRNA in ovarian stroma and follicles of geese

In all the experimental follicles and ovarian stroma, *OAZ1* transcripts were detectable (Fig. 4). As the follicle size increased, except for F5 and F2 follicles, the level of the *OAZ1* mRNA expression increased during follicular development, while it decreased during follicular regression. Except for the F5 follicle, the level of *OAZ1* mRNA expression in preovulatory follicles was significantly higher than that of the SWF ($P < 0.05$). The level of *OAZ1* mRNA expression was the lowest in the F5 follicle, and was 0.65-fold compared to that in SWF ($P < 0.05$). *OAZ1* mRNA expression in the F1 follicle was 2.11-fold compared to that in SWF ($P < 0.05$). It was the highest in POF1 in all of the examined tissues, and was 2.49-fold higher than that in SWF ($P < 0.05$). However, the level of *OAZ1* mRNA expression among POF2, POF3 and POF4 follicles was not significantly different ($P > 0.05$). The expression level of *OAZ1* between the ovarian stroma and the SWF follicles was not significantly different ($P > 0.05$).

4. Discussion

As introduced previously, a full-length *OAZ1* coding sequence of the Sichuan white goose was obtained and sequenced for verification. Like all other members of the *OAZ* gene family [10], the goose *OAZ1* was also encoded by two overlapping ORFs with a conserved $+1$ ribosomal frameshift positioned at $+175$. Once again, our results
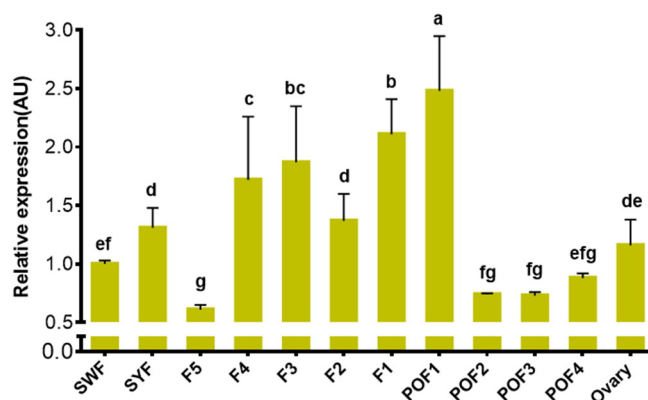

Fig. 4. Expression levels of the *OAZ1* gene in ovarian stroma and follicles of the Sichuan white goose. The level of the *OAZ1* gene expression were normalized to *GAPDH*. Expression levels calculated by the $2^{-\Delta\Delta Ct}$ method are presented in AU. The significance of differences in the expression levels of *OAZ1* gene was determined by one-way ANOVA, followed by Duncan's multiple range test. Data are presented as mean $\pm$ SEM. Bars without a common letter are significantly different ($P < 0.05$).

consolidated that $+1$ frameshift at the end of ORF1 was required for the expression of the full-length protein [16]. Compared to the amino acid sequence of ORF1, the goose ORF2 amino acid sequence shared higher similarity with that in mammalian species. Ichiba et al. [22] constructed a series of deletion mutants (*OAZ1* 69-227) of rat *OAZ1* cDNAs, and indicated that this region had all of the known functions of *OAZ*, such as its binding to ODC and inhibition of its activity and destabilization [22,23]. Furthermore, OAZ1 retains normal functions even after truncation of amino acids 1–68. Thus, it is not surprising that the similarity of the amino acid sequence of ORF2 was highly conserved, while that of ORF1 was conserved to a lesser extent. Ten amino acid residues (TLHASR and RGGS/C/R) in the ORF1 of OAZ1 in birds were deleted compared to mammals. Whether these 10 deleted amino acid residues in birds have any functions remains to be determined. Furthermore, the similarity of OAZ1 amino acid sequences among birds remained at 99%, while it was around 80% among mammals. This indicates that the function of OAZ1 differ between birds and mammals. Three potential domains (OAZ domain, signature and super family domain) were mainly located in the ORF2 of the goose OAZ1. It reinforced that ORF2 of OAZ1 was essential for the distinguishable activities, such as binding to and inhibiting ODC; acceleration of ODC degradation by the 26S proteasome; and inhibition of intracellular polyamine uptake [24,25]. In rats, two regions of OAZ1 (amino acids 122–144 and 211–218) are necessary for its binding to
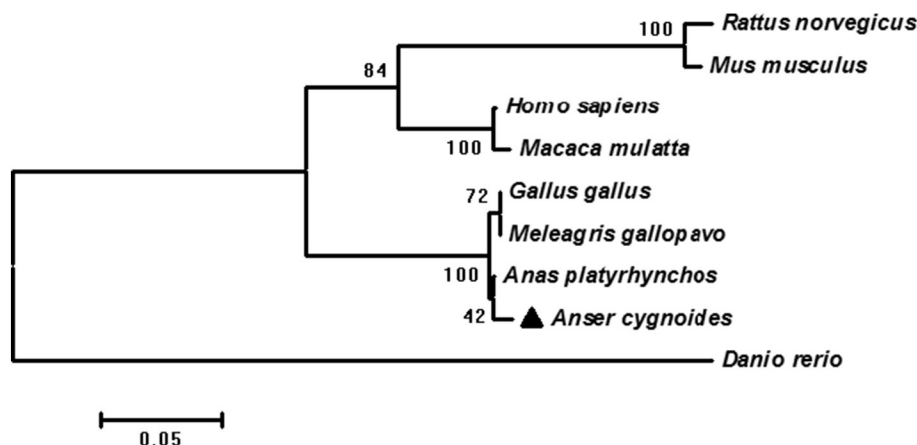

Fig. 3. Phylogenetic tree of OAZ1 amino acid sequences from different species. Neighbor-joining analysis based on the Poisson correction model with 1000 bootstrap replicates was performed using Mega 5.20 software. Numbers at each branch indicate the percentage of times a node was supported in 1000 bootstrap replicates. The species names and GenBank accession numbers of the OAZ1 sequences shown were as follows: *A. platyrhynchos* (NP_001276770), *G. gallus* (NP_990247), *M. gallopavo* (NP_001278810), *H. sapiens* (NP_004143), *Macaca mulatta* (NP_001128372), *M. musculus* (NP_032779), *R. norvegicus* (NP_620781) and *D. rerio* (NP_919413).

ODC and inhibition of its activity, and an additional region (amino acids 88–118, especially 113–118) is necessary for its destabilization [22]. However, it is noteworthy that the region (amino acids 122–144) of OAZ1 in birds shared lower similarity to that in mammals. This lower conserved region may alter the ability of avian OAZ1 binding to ODC and inhibiting ODC activity. It is not certain, however, whether the effect will be enhancement or attenuation. In addition, except for *Danio rerio*, the first 23 residues of the OAZ1 amino acid sequence was highly conserved in these compared species. Thus, further studies are warranted to clarify whether these highly identified residues may contribute to certain functions of OAZ1.

The molecular weight of the purified OAZ1 from rat liver was determined to be 22.0 kDa using gel filtration on Sephadex G-75 and 19.0 kDa using SDS-PAGE [26]. In our study, the molecular mass of the goose OAZ1 protein was predicted to be 24.37 kDa. The purified OAZ1 from the birds remains to be identified. The polyamines, which are essential for cell proliferation and differentiation, have a wide tissue distribution in mammals. The OAZ1 protein is distributed in mitochondria, cell nuclei, cytoplasm, extracellularly (including cell wall) and the cytoskeleton in the goose. Along with our previous study [27], these results show that OAZ1 distribution is ubiquitous in various tissues as well as cellular compartments.

OAZ1, which is a regulator for ODC activity and polyamine transport, is essential for maintaining polyamine homeostasis. In the present study, significant difference in *OAZ1* abundance among ovarian and follicular tissues suggests that *OAZ1* expression and distribution is tissue specific. This is consistent with the study of Yi et al. [27], in which *OAZ1* was ubiquitously expressed in a tissue-specific manner in the Sichuan white goose. These results suggest that *OAZ1* is ubiquitously and tissue-specifically expressed in various tissues of geese. However, de Jonge et al. [28] reported that *OAZ1* gene was stably expressed in different cellular and experimental contexts in mice. Furthermore, Piorkowska et al. [29] showed that *OAZ1* were stably expressed in porcine backfat tissue across different breeds. Thus, stable expression of *OAZ1* mRNA may be differ among various species and tissues.

The blockade of ovarian ODC by α-difluoromethylornithine could inhibit ovarian growth, folliculogenesis and formation of Graafian follicles [30]. Our previous results indicated that ODC activity mediated by OAZ1 might regulated the process of follicular development [18]. Among preovulatory follicles, the level of *OAZ1* mRNA expression was lowest in the F5 follicle ($P < 0.05$). The F5 follicle, which is the first preovulatory hierarchal follicles selected from SYF, begins the process of growth and differentiation. This process is a rapid phase of growth compared with SWF. Decreased expression of *OAZ1* mRNA can increase ODC activity and polyamine biosynthesis, and then promote the growth of ovarian follicles. *OAZ1* abundance showed an increasing trend during follicular development, while it decreased during follicular regression. *OAZ1* mRNA expression in the F1 follicle was 2.11-fold compared to that in the SWF ($P < 0.05$). Increased *OAZ1* expression not only inhibited theca and granulosa cell proliferation by blocking polyamine biosynthesis, but also regulated apoptosis through decreasing the activity of Cyclin-D1 and Smad1 [31]. Thus, proliferation of theca and granulosa cells and incorporation of lipoprotein-rich yolk are slow in the F1 follicle. At the time of ovulation, certain selective cells within the stigma region die via apoptosis. More cell death via apoptosis is initiated shortly after ovulation, and the POF follicle is largely reabsorbed within several days. The present result shows *OAZ1* expression in the POF1 follicle was the highest among all of the examined tissues ($P < 0.05$). Thus, we speculate that increasing *OAZ1* expression level accelerates the depletion of intracellular polyamines, and promotes theca and granulosa cell apoptosis and regression of the POF follicle.

5. Conclusions

We have reported the cDNA sequence of goose *OAZ1* and its characteristics. *OAZ1* is expressed ubiquitously and in a tissue-specific

manner in various tissues of geese. The present study provides an evidence for a potential function of OAZ1 in follicular development, ovulation and regression, and strengthens the hypothesis of a link between polyamines and ovarian functions in geese.

Conflict of interest

The authors declare that they have no conflict of interest.

The nucleotide sequence reported in this paper has been deposited in the NCBI/GenBank Data Libraries under the accession number KC845302.

References

[1] Pegg AE. Mammalian polyamine metabolism and function. IUBMB Life 2009;61:880–94. http://dx.doi.org/10.1002/iub.230.
[2] Igarashi K, Kashiwagi K. Modulation of protein synthesis by polyamines. IUBMB Life 2015;67:160–9. http://dx.doi.org/10.1002/iub.1363.
[3] Lefevre PL, Palin MF, Murphy BD. Polyamines on the reproductive landscape. Endocr Rev 2011;32:694–712. http://dx.doi.org/10.1210/er.2011-0012.
[4] Li WD, Huang M, WG Lu, Chen X, Shen MH, Li XM, et al. Involvement of antizyme characterized from the small abalone *Haliotis Diversicolor* in gonadal development. PLoS One 2015;10:e0135251. http://dx.doi.org/10.1371/journal.pone.0135251.
[5] Ma R, Jiang D, Kang B, Bai L, He H, Chen Z, et al. Molecular cloning and mRNA expression analysis of antizyme inhibitor 1 in the ovarian follicles of the Sichuan white goose. Gene 2015;568:55–60. http://dx.doi.org/10.1016/j.gene.2015.05.014.
[6] Fenelon JC, Banerjee A, Lefevre P, Gratian F, Murphy BD. Polyamine-mediated effects of prolactin dictate emergence from mink obligate embryonic diapause. Biol Reprod 2016;95:1–13. http://dx.doi.org/10.1095/biolreprod.116.139204.
[7] Di Martino ML, Campilongo R, Casalino M, Micheli G, Colonna B, Prosseda G. Polyamines: Emerging players in bacteria-host interactions. Int J Med Microbiol 2013;303:484–91. http://dx.doi.org/10.1016/j.ijmm.2013.06.008.
[8] Pegg AE. Regulation of ornithine decarboxylase. J Biol Chem 2006;281:14529–32. http://dx.doi.org/10.1074/jbc.R500031200.
[9] Nowotarski SL, Shantz LM. Cytoplasmic accumulation of the RNA-binding protein HuR stabilizes the ornithine decarboxylase transcript in a murine nonmelanoma skin cancer model. J Biol Chem 2010;285:31885–94. http://dx.doi.org/10.1074/jbc.M110.148767.
[10] He H, Kang B, Jiang D, Ma R, Bai L. Molecular cloning and mRNA expression analysis of ornithine decarboxylase antizyme 2 in ovarian follicles of the Sichuan white goose (*Anser cygnoides*). Gene 2014;545:247–52. http://dx.doi.org/10.1016/j.gene.2014.05.022.
[11] Tajima A, Murai N, Murakami Y, Iwamoto T, Migita T, Matsufuji S. Polyamine regulating protein antizyme binds to ATP citrate lyase to accelerate acetyl-CoA production in cancer cells. Biochem Biophys Res Commun 2016;471:646–51. http://dx.doi.org/10.1016/j.bbrc.2016.02.084.
[12] Matsufuji S, Matsufuji T, Miyazaki Y, Murakami Y, Atkins JF, Gesteland RF, et al. Autoregulatory frameshifting in decoding mammalian ornithine decarboxylase antizyme. Cell 1995;80:51–60. http://dx.doi.org/10.1016/0092-8674(95)90450-6.
[13] Bunjobpol W, Dulloo I, Igarashi K, Concin N, Matsuo K, Sabapathy K. Suppression of acetylpolyamine oxidase by selected AP-1 members regulates DNp73 abundance: Mechanistic insights for overcoming DNp73-mediated resistance to chemotherapeutic drugs. Cell Death Differ 2014;21:1240–9. http://dx.doi.org/10.1038/cdd.2014.41.
[14] Mangold U. The antizyme family: Polyamines and beyond. IUBMB Life 2005;57:671–6. http://dx.doi.org/10.1080/15216540500307031.
[15] Childs AC, Mehta DJ, Gerner EW. Polyamine-dependent gene expression. Cell Mol Life Sci 2003;60:1394–406. http://dx.doi.org/10.1007/s00018-003-2332-4.
[16] Kurian L, Palanimurugan R, Godderz D, Dohmen RJ. Polyamine sensing by nascent ornithine decarboxylase antizyme stimulates decoding of its mRNA. Nature 2011;477:490–4. http://dx.doi.org/10.1038/nature10393.
[17] HY Wu, Chen SF, Hsieh JY, Chou F, Wang YH, Lin WT, et al. Structural basis of antizyme-mediated regulation of polyamine homeostasis. Proc Natl Acad Sci U S A 2015;112:11229–34. http://dx.doi.org/10.1073/pnas.1508187112.
[18] Kang B, Guo JR, Yang HM, Zhou RJ, Liu JX, Li SZ, et al. Differential expression profiling of ovarian genes in prelaying and laying geese. Poult Sci 2009;88:1975–83. http://dx.doi.org/10.3382/ps.2008-00519.
[19] An XP, Hou JX, Li G, Peng JY, Liu XQ, Liu HY, et al. Analysis of differentially expressed genes in ovaries of polytocous versus monotocous dairy goats using suppressive subtractive hybridization. Reprod Domest Anim 2012;47:498–503. http://dx.doi.org/10.1111/j.1439-0531.2011.01910.x.
[20] Kang B, Jiang DM, Bai L, He H, Ma R. Molecular characterisation and expression profiling of the *ENO1* gene in the ovarian follicle of the Sichuan white goose. Mol Biol Rep 2014;41:1927–35. http://dx.doi.org/10.1007/s11033-014-3039-3.

[21] Tamura K, Stecher G, Peterson D, Filipski A, Kumar S. MEGA6: Molecular evolutionary genetics analysis version 6.0. Mol Biol Evol 2013;30:2725–9. http://dx.doi.org/10.1093/molbev/mst197.

[22] Ichiba T, Matsufuji S, Miyazaki Y, Murakami Y, Tanaka K, Ichihara A, et al. Functional regions of ornithine decarboxylase antizyme. Biochem Biophys Res Commun 1994;200:1721–7. http://dx.doi.org/10.1006/bbrc.1994.1651.

[23] Li X, Coffino P. Distinct domains of antizyme required for binding and proteolysis of ornithine decarboxylase. Mol Cell Bioll 1994;14:87–92. http://dx.doi.org/10.1128/mcb.14.1.87.

[24] Saito T, Hascilowicz T, Ohkido I, Kikuchi Y, Okamoto H, Hayashi S, et al. Two zebrafish (Danio rerio) antizymes with different expression and activities. Biochem J 2000;345:99–106. http://dx.doi.org/10.1042/bj3450099.

[25] Ramos-Molina B, Lopez-Contreras AJ, Lambertos A, Dardonville C, Cremades A, Peñafiel R. Influence of ornithine decarboxylase antizymes and antizyme inhibitors on agmatine uptake by mammalian cells. Amino Acids 2015;47:1025–34. http://dx.doi.org/10.1007/s00726-015-1931-3.

[26] Kitani T, Fujisawa H. Purification and some properties of a protein inhibitor (antizyme) of ornithine decarboxylase from rat liver. J Biol Chem 1984;259:10036–40.

[27] Yi ZX, Jiang DM, Kang B. Study on differential expression of OAZ1 and OAZ2 gene in various tissues of Sichuan white goose. Acta Bot Boreali-Sin 2014;29:50–4. http://dx.doi.org/10.7668/hbnxb.2014.01.010.

[28] De Jonge HJ, Fehrmann RS, De Bont ES, Hofstra RM, Gerbens F, Kamps WA, et al. Evidence based selection of housekeeping genes. PLoS One 2007;2:e898. http://dx.doi.org/10.1371/journal.pone.0000898.

[29] Piorkowska K, Oczkowicz M, Rozycki M, Ropka-Molik K, Piestrzynska-Kajtoch A. Novel porcine housekeeping genes for real-time RT-PCR experiments normalization in adipose tissue: Assessment of leptin mRNA quantity in different pig breeds. Meat Sci 2011;87:191–5. http://dx.doi.org/10.1016/j.meatsci.2010.10.008.

[30] Bastida CM, Cremades A, Castells MT, Lopez-Contreras AJ, Lopez-Garcia C, Tejada F, et al. Influence of ovarian ornithine decarboxylase in folliculogenesis and luteinization. Endocrinology 2005;146:666–74. http://dx.doi.org/10.1210/en.2004-1004.

[31] Gruendler C, Lin Y, Farley J, Wang T. Proteasomal degradation of Smad1 induced by bone morphogenetic proteins. J Biol Chem 2001;276:46533–43. http://dx.doi.org/10.1074/jbc.M105500200.